# Head Tracking Three-Dimensional Integral Imaging Display Using Smart Pseudoscopic-to-Orthoscopic Conversion

Xin Shen, Manuel Martinez Corral, and Bahram Javidi, *Member, IEEE*

***Abstract*—A novel head tracking three-dimensional (3D) integral imaging display is presented. By means of proper application of the smart pseudoscopic-to-orthoscopic conversion (SPOC) method, our display allows an extended viewing angle accommodated to the viewer's position which is obtained by a head/eye tracking system. Using the SPOC, new sets of elemental images are calculated and adapted to any specific viewing position. Additionally, the crosstalk which is typical in conventional integral imaging, is eliminated for a large viewing angle. By performing the rotation transformation in the simulated display, viewing a 3D scene with head rotation can be realized for robust display. Experimental results verify the feasibility of our proposed method.**

***Index Terms*—Head tracking, integral imaging, smart pseudoscopic-to-orthoscopic conversion, 3D display.**

## I. Introduction

INTEGRAL IMAGING [1] is a very promising three-dimensional (3D) technology which has drawn substantial interest for 3D TV and displays [2]–[14]. Integral imaging offers many advantages such as continuous viewing points and visualization without special viewing glasses, etc. One of its shortcomings is the limited viewing angle of the 3D display. The viewing angle or field of view of a conventional integral imaging display mainly depends on the f-number of the lenslet and the distance between the lenslet and the display screen. If an observer views the 3D image with a viewing angle that exceeds the field of view of the display, the quality of the 3D image will be degraded. Many works have been done to analyze and solve this problem [15]–[18].

In this paper, we propose a novel head tracking 3D integral imaging display for extended viewing angle and 3D scene rotation by utilizing the pseudoscopic-to-orthoscopic conversion (SPOC). The SPOC method [21]–[23] was proposed for the 3D image transformation from pseudoscopic to orthoscopic format with full control over the display parameters. With this method, we are able to computationally generate a new set of elemental images from the real captured elemental images for head tracking 3D display. Instead of using computer software to only generate virtual 3D scenes, the proposed method can be used for real time head tracking integral imaging [24]–[26] for both real and virtual 3D scenes.

For the SPOC in integral imaging, the conventional real captured 3D scene [19], [20] is recorded by a set of 2D images, which are referred to as the captured elemental images [21]. The captured elemental images will first be virtually reconstructed in the 3D space. Considering the parameters of the display system, a virtual pinhole array will be set for capturing the virtually reconstructed image. A new set of elemental images for head tracking 3D display corresponding to the specific viewing position will be generated. The head tracking 3D display can eliminate the crosstalk problem for the observation with a large viewing angle. This allows for an improvement of the viewing angle without any additional optical equipment. In addition, by utilizing the image transformation in the proposed method, the visualization of rotated 3D scene can be computationally calculated corresponding to the rotation degree of the observer's head. Experimental results show the feasibility of our proposed method. We believe that the 3D display with head tracking has a wide range of applications for head mounted display, augmented reality, etc [28].

This paper first derives the viewing angle of a conventional integral imaging display and head tracking integral imaging with a specific viewing position. Then the proposed method is explained to generate a new set of elemental images for head tracking 3D display, along with the details of the 3D display experimental results. Conclusions are given in the end of this paper.

## II. Viewing Angle of Integral Imaging Display

For the conventional integral imaging display, the viewing angle is based on the parameters of the 3D display system. As shown in Fig. 1(a), an observer is able to view high quality 3D image within the viewing zone. The viewing angle of the system is [27]

$$\theta_1 = 2\arctan\left(\frac{p}{2g}\right) \tag{1}$$

Manuscript received September 07, 2015; revised November 14, 2015; accepted December 04, 2015. Date of publication December 08, 2015; date of current version May 09, 2016. This work was supported in part by the Samsung Advanced Institute of Technology (SAIT) Global Research Outreach (GRO) Program and the National Science Foundation under Grant NSF NSF/IIS-1422179. The work of M. Martinez-Corral was supported in part by the Spanish Ministry of Economy under Grant DPI2012-32994 and the Generalitat Valenciana under Grant PROMETEOII/2014/072.

X. Shen and B. Javidi are with the Electrical and Computer Engineering Department, University of Connecticut, Storrs, CT 06269 USA. (e-mail: xin.shen@uconn.edu; bahram.javidi@uconn.edu).

Manuel Martinez-Corral is with the Department of Optics, University of Valencia, E-46100 Burjassot, Spain (e-mail: Manuel.Martinez@uv.es).

Color versions of one or more of the figures are available online at http://ieeexplore.ieee.org.

Digital Object Identifier 10.1109/JDT.2015.2506615

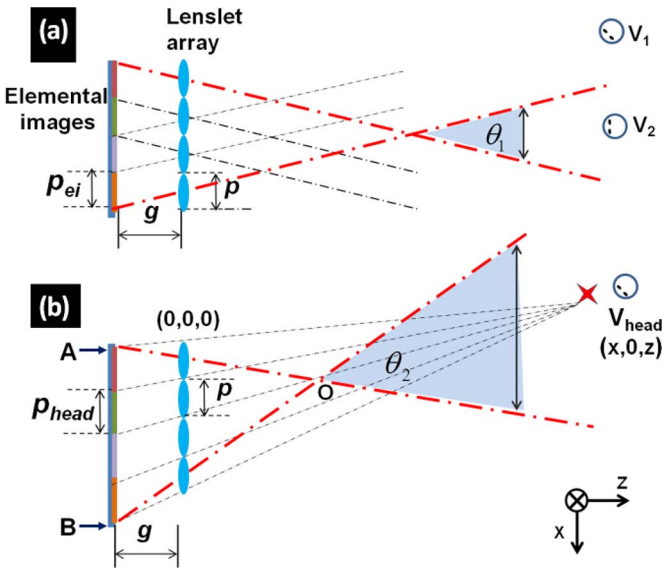


Fig. 1. Viewing angle of an integral imaging display. (a) For the conventional integral imaging. (b) For the head tracking integral imaging with a specific viewing position. $p$ is the pitch of the lenslet, $p_{ei}$ and $p_{\mathrm{head}}$ are the elemental image size of conventional and head tracking display, respectively. $\theta_1$ and $\theta_2$ are the viewing angle of conventional and head tracking integral imaging, respectively.

where $p$ is the pitch of the lenslet, $g$ is the distance between the elemental images and their corresponding lenslets. To avoid the crosstalk, the size of each elemental image $(p_{ei})$ is identical to the pitch of the lenslet $(p)$.

However, if the observer watches the 3D image with a large viewing angle, such as at the viewing position of $V_1$ in Fig. 1(a), the viewing angle will exceed the field of view of the system. In this case, pixels from the adjacent elemental images will pass through the lenslet and integrate in the 3D space as a 3D image. Due to the crosstalk, the 3D display quality may be degraded substantially because of the flipped 3D images.

To provide high quality 3D display with a large viewing angle, we utilize the head tracking technology for integral imaging display [29]. With an image sensor and head/eye tracking software, the viewing parameters in the 3D space can be obtained. A new set of elemental images corresponding to the detected viewing position needs to be generated for head tracking 3D display. As shown in Fig. 1(b), the original coordinate is set to the top left of the lenslet array. By fully utilizing the lenslets, the viewing angle of head tracking integral imaging with the specific viewing position $V_{\mathrm{head}}(\mathrm{x},0,\mathrm{z})$, can be expressed as

$$\begin{aligned}\theta_2 &= \angle AOB \\ &= \arctan\left|\frac{4gpz^2+4g^2npz}{4g^2z^2-p^2z^2-2np^2gz-4npg^2x+4g^2x^2}\right| \end{aligned} \tag{2}$$

where $p$ is the pitch of the lenslet, $n$ is the number of the lenslets in the $x$ axis, $(x,0,z)$ is the coordinate of the viewing position and $g$ is the distance between the elemental image and the lenslet. $A$ and $B$ are the first and last pixel on the elemental image plane, respectively. $O$ is the point intersection between the lines for the edges of the field of view.

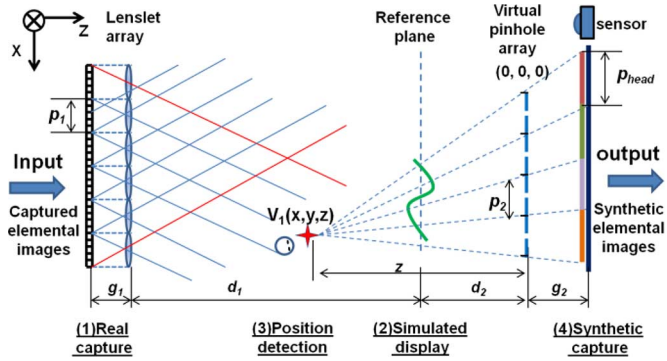


Fig. 2. Generation of synthetic elemental images for head tracking integral imaging display.

The size (mm) and resolution (pixel) of each elemental image for the head tracking 3D display are denoted as $p_{\mathrm{head}}$ and $r_{\mathrm{head}}$, respectively, which can be expressed as:

$$p_{\mathrm{head}} = p\left(1+\frac{g}{z}\right), \tag{3}$$

$$r_{\mathrm{head}} = \frac{p_{\mathrm{head}}}{s_{\mathrm{pixel}}} = \frac{p\,(1+g/z)}{s_{\mathrm{pixel}}} \tag{4}$$

where $s_{\mathrm{pixel}}$ is the pixel size (mm/pixel).

Comparing with the elemental image size $(p_{ei})$ for conventional integral imaging discussed before, the size of each head tracking elemental image $(p_{\mathrm{head}})$ has an additional part of $p \times g/z$, which also depends on the observation distance $(z)$ and the parameter of the display system $(g)$. By correct pixel mapping, the newly generated elemental images can be integrated into 3D images for the specific viewing position without crosstalk to avoid the flipped images. For a virtual 3D scene, computer software can generate new elemental images corresponding to any specific viewing angle [17]. However, for a practical real 3D scene, it is not possible to pre-capture various sets of elemental image arrays with different perspectives. We propose the head tracking synthetic capture method to generate elemental images for 3D integral imaging with specific viewing position.

## III. Head Tracking Integral Imaging Display Using Pseudoscopic-to-Orthoscopic Conversion Method

Fig. 2 illustrates the principle of the proposed method to generate new set of elemental images for head tracking 3D display. The original coordinate is set to the top left of the virtual pinhole array. The proposed method includes four general stages: (1) real capture; (2) simulated display; (3) viewing position detection; and (4) head tracking synthetic capture. A set of 2D images, referred to as captured elemental images, are first captured by the conventional integral imaging pickup system. A lenslet array or camera array can be used for the real capture. The captured elemental images are the input to the proposed method and the optical axes in the real capture are parallel with each other. Secondly, the captured elemental images will be computationally reconstructed in the virtual 3D space. A reference plane (RP) is selected at the distance $d_1$ from the lenslet array corresponding to the depth of the 3D scene for simulated display.

The simulated display is the computational reconstruction of integral imaging, so that the reference plane can be regarded as the reconstruction plane. The pixel intensity on the reference plane can be calculated by the computational reconstruction process shown in (5) at the bottom of the page [11], [13], where $(x, y)$ is the pixel index on the reference plane, $M$ and $N$ are the number of the lenslet in the $x$ and $y$ axes, $M_0 = d_1/g_1$ is the magnification factor, $(S_x^{ij}, S_y^{ij})$ is the position of the $ij$th lenslet.

The detection of the viewing position can be obtained by a commercial head/eye detection system, which contains an image sensor and feature detection software. For the head tracking synthetic capture stage, a new set of elemental images, called synthetic elemental images, is generated corresponding to the detected viewing position. A virtual pinhole array is set in the 3D space for the synthetic capture. As the capture and display of integral imaging is a pair of inverse processes, the parameters of the virtual pinhole array should be identical to the display system to match the format of 3D display [30], [31]. The distance $(d_2)$ between the reference plane and the virtual pinhole array depends on the depth range of the display system. The distance $(g_2)$ between the virtual pinholes and the synthetic elemental images depends on the focal length of the lenslet array in the 3D display. Also, the pitch $(p_2)$ of the virtual pinhole is identical to the pitch of the lenslet used for the 3D display. The size and resolution of the synthetic elemental images can be calculated by (3) and (4), based on the parameters of the viewing position and the display system.

To further explain the synthetic capture, we first calculate the region for each of the synthetic elemental images. For simplification, two dimensional ($x$-$z$ axes) case is taken into consideration. The original position is set on the top of the virtual pinhole array as (0, 0, 0), as shown in Fig. 2. An image sensor is used for detecting the viewing position. Let us assume that the detected viewing position is at $V_1(x, 0, z)$ and a total of K virtual pinholes are set in the 3D space. The coordinate of the first pixel for each synthetic elemental image (SEI) is

$$SEI_i^1 = (i-1) \times p_2 - g_2 \times \left[ \frac{x - (i-1) \times p_2}{z} \right] \quad (6)$$

where $i$ is the index of virtual pinholes, $p_2$ is the pitch of the virtual pinhole, and $g_2$ is the distance between the virtual pinhole and the synthetic elemental image.

Once the positions of the first pixels $(SEI_i^1)$ for each synthetic elemental image are obtained, the synthetic elemental image plane can be classified into K groups corresponding to the K

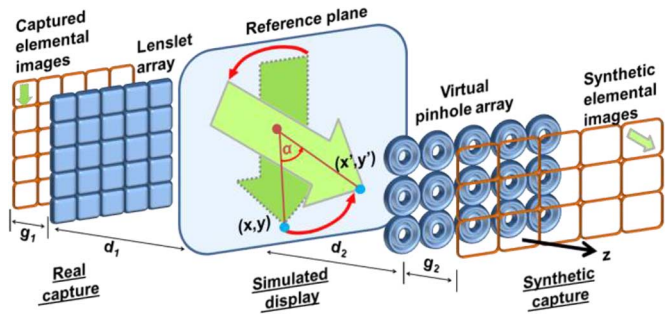


Fig. 3. Generation of synthetic elemental images with 3D scene rotation.

pinholes. The last step for the synthetic capture is the pixel mapping between the synthetic elemental image (SEI) plane and the reference plane. Based on the pinhole model, the pixel coordinate $(x_j^{RP})$ on the reference plane corresponding to the $j$th pixel on the SEI plane can be described as given by (7), shown at the bottom of the page, where $j$ is the pixel index on the synthetic elemental image plane, $\lfloor . \rfloor$ is the floor operation for the index of the synthetic elemental images, $SEI_1^1$ is the coordinate of the first pixel on the synthetic elemental image plane which can be obtained by (6). $p_{\text{head}}$ and $r_{\text{head}}$ can be calculated by (3) and (4). We are able to obtain the pixel coordinate for the y axis $(y_j^{RP})$ in the same way. Combining (5)–(7), the pixel mapping between the real captured elemental images and the synthetic elemental images are realized. Thus, the new set of elemental images for head tracking integral imaging is generated.

In some cases, the viewing position $(x, y, z, \alpha)$ may also have a rotation degree of $\alpha$. To display 3D images corresponding to observer's head movement, it is necessary to discuss the integral imaging with 3D scene rotation for accommodating viewing the 3D scene. As the real captured elemental images contain multiple perspectives to the 3D scene, it is impossible to display rotated 3D scenes by rotation of the elemental image directly. With SPOC method, it is possible to solve the problem and realize the 3D scene rotation for head tracking 3D display. As shown in Fig. 3, once the head rotation degree is obtained, we can implement the rotation transformation on the simulated display stage. The inverse transformation to the image rotation is

$$\begin{bmatrix} \cos(\alpha) & -\sin(\alpha) \\ \sin(\alpha) & \cos(\alpha) \end{bmatrix} \begin{bmatrix} x' \\ y' \end{bmatrix} = \begin{bmatrix} x \\ y \end{bmatrix} \quad (8)$$

where $\alpha$ is the rotation degree of the viewing point, which can be detected by a head/eye tracking system, $(x, y)$ is the original pixel coordinate on the reference plane, and $(x', y')$ is the new

$$RP(x, y, d_1) = \frac{1}{MN} \sum_{i=1}^{M} \sum_{j=1}^{N} EI^{ij} \left( \mathrm{x} + \frac{1}{M_0} S_x^{ij}, \mathrm{y} + \frac{1}{M_0} S_y^{ij} \right) \quad (5)$$

$$x_j^{RP} = \frac{\left[ (j \times p_{\text{head}}) - SEI_1^1 - \left( \left\lfloor \frac{j}{r_{\text{head}}} \right\rfloor \times p_2 + \frac{p_2}{2} \right) \right] \times d_2}{g_2} + \left( \left\lfloor \frac{j}{r_{\text{head}}} \right\rfloor \times p_2 + \frac{p_2}{2} \right) \quad (7)$$

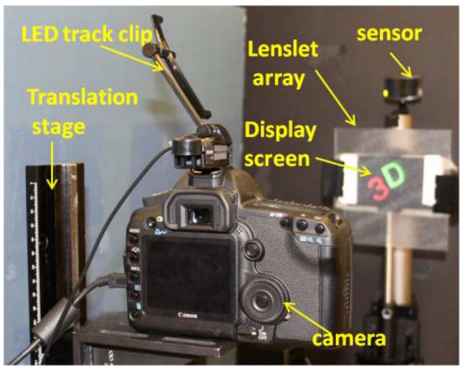


Fig. 4. Experimental setup for the head tracking 3D display.

pixel coordinate after 3D scene rotation. We can combine (5) and (8) to achieve the pixel mapping between the real captured elemental images and the reference plane with 3D scene rotation. The new set of elemental images with 3D rotation can be generated by the synthetic captured stage as discussed before.

## IV. 3D Integral Imaging Experimental Display Results

To show the feasibility of our proposed methods, conventional and head tracking integral imaging experiments using SPOC were implemented. A smart phone (HTC-One) and lenslet array were used as a 3D display system. A digital camera (Canon 5D) was used as an observer and placed at different viewing positions. A head tracking device TrackIR 5.2™ includes an LED track clip and a head tracking sensor was used in the experiments. The position of the LED track clip was affiliated with the camera, and the sensor was located on the display plane to obtain the viewing position.

A 3D scene was generated by software (3dsMax), and the captured elemental images were obtained by the synthetic aperture integral imaging technique [32]. The 3D scene consists of characters "3" and "D", which are located at 40 mm and 60 mm from the lenslet array, respectively. A total of 7 (H) $\times$ 7 (V) elemental images were obtained, and the distance $(g_1)$ between the captured elemental images and the lenslet array was 6.01mm. The reference plane was set in the center of the 3D scene ($d_1 = 50$ mm) for the simulated display.

The resolution of the display screen (HTC-One) is 1920 (H) $\times$ 1080 (V) pixels with the pixel size of $\sim$54 $\mu$m. The pitch of the lenslet is 1 mm, and the distance $(g_2)$ between the lenslet array and the display screen is 3.3 mm. A set of 104 (H) $\times$ 58 (V) synthetic elemental images was generated. The resolution of each elemental image is 18 (H) $\times$ 18 (V) pixels. The parameters for the synthetic capture are based on the 3D display system. We set the distance $(d_2)$ between the reference plane and the virtual pinhole array as 20 mm. As a result, the 3D image can be displayed around 20 mm from the lenslet array.

Fig. 4 illustrates the experimental setup. The specifications of the real capture and synthetic capture for the head tracking experiments are shown in Table I.

The center of the display screen is set as the viewing center for calculating the viewing angle. The viewing angle for the conventional integral imaging display in our experiments is

TABLE I
Specifications of the Real Capture and Synthetic Capture for the Experiments

| Specifications | Real capture | Synthetic capture |
|---|---|---|
| $g$ (mm) | 6.03 ($g_1$) | 3.30 ($g_2$) |
| $d$ (mm) | 50 ($d_1$) | 20 ($d_2$) |
| Elemental images (EI) | 7 (H) × 7 (V) | 104 (H) × 58(V) |
| Size of EI (mm) | 5 × 5 | 1 × 1 |
| Resolution of EI (pixel) | 2000 × 2000 | 18 × 18 |

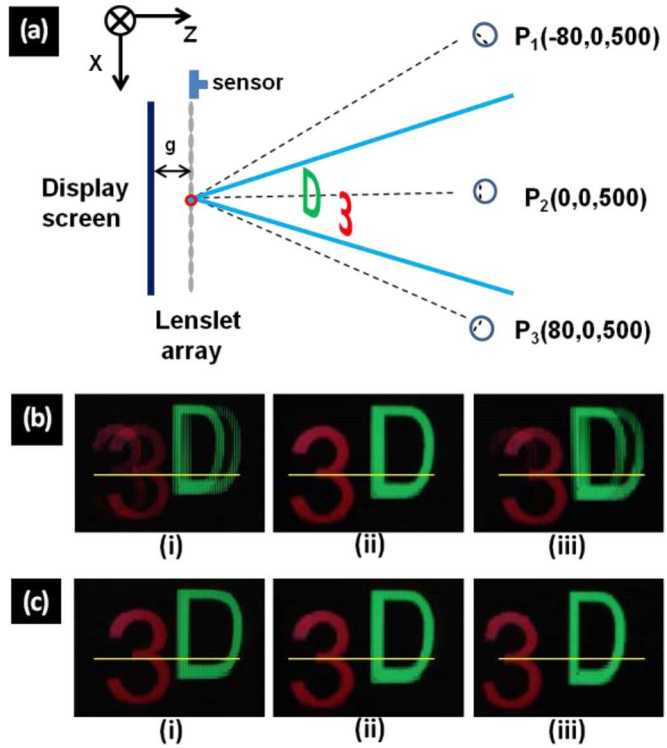


Fig. 5. (a) 3D display with different viewing positions (left view $P_1$, center view $P_2$ and right view $P_3$). Display results with (b) conventional integral imaging, and (c) head tracking integral imaging. Observed display results from (i) left view, (ii) center view, and (iii) right view. The original coordinate is set to the top center of the lenslet array.

$17.2°(\pm 8.6°)$. If an observer views the 3D image with an even larger viewing angle, the display results will be degraded with flipped 3D images due to the crosstalk. Fig. 5(a) illustrates the head tracking experiments with different viewing positions.

In the experiments, the camera was first placed at three different viewing positions corresponding to the left perspective $P_1$ $(-80, 0, 500)$, center perspective $P_2$ $(0, 0, 500)$ and right perspective $P_3$ (80, 0, 500), in front of the 3D display. The specifications are illustrated in Table II. The viewing positions $P_1$ and $P_3$ have a viewing angle of $(\pm)$ 9.1° which are out of the acceptable viewing angle for the conventional integral imaging. The observed 3D images are flipped because of the crosstalk, as shown in Fig. 5(b), (i) and (iii), respectively. By using the proposed method, two new sets of elemental images are generated for the observer at $P_1$ and $P_3$, respectively. The display results are improved without image flipping, as shown in Fig. 5(c), (i) and (iii) for the viewing positions of $P_1$ and $P_3$, respectively. When the observer watches the 3D display from the center position, $P_2$, which is in the acceptable viewing angle of the con-

TABLE II
SPECIFICATIONS OF THE HEAD TRACKING EXPERIMENTS WITH DIFFERENT VIEWING POSITIONS. 'IN' INDICATES THAT THE RECONSTRUCTION IS WITHIN THE FIELD OF VIEW

| Observation | | Integral Imaging | | | |
|---|---|---|---|---|---|
| Viewing position (mm) | Viewing angle | Conventional (±8.6°) | Head tracking | | |
| | | | $P_1$ | $P_2$ | $P_3$ |
| $P_1$(−80, 0, 500) | −9.1° | Distorted | In | | |
| $P_2$ (0, 0, 500) | 0 | In | | In | |
| $P_3$ (80, 0, 500) | 9.1° | Distorted | | | In |

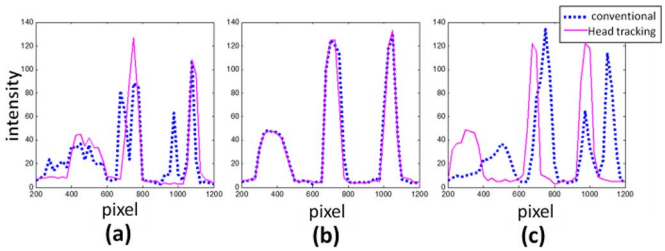


Fig. 6. 1D intensity profiles along the yellow lines in Fig. 5(b) and (c) to illustrate the comparison between the display results of the conventional and head tracking integral imaging. (a) Left view. (b) Center view. (c) Right view.

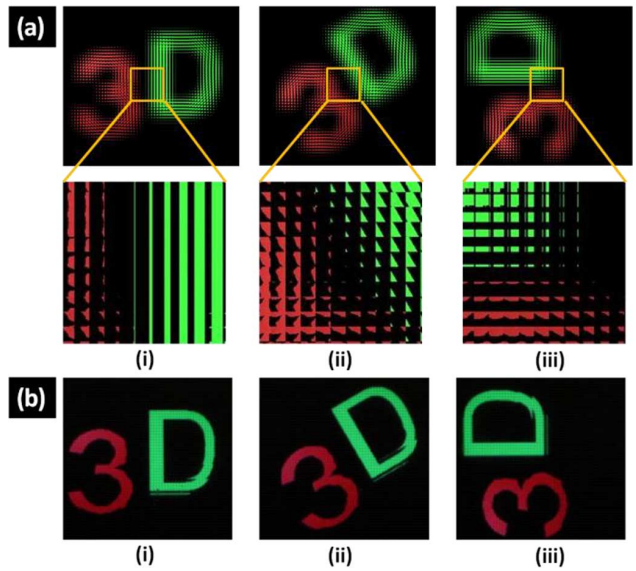


Fig. 7. Experimental results for viewer head rotation. (a) Generated synthetic elemental images and (b) the 3D display results with rotation degrees of (i) 0°, (ii) 30°, and (iii) 90°.

ventional integral imaging, both of the conventional and head tracking sets of elemental images provide high quality of 3D reconstruction, as shown in (ii) of Fig. 5(b) and (c), respectively. Comparing the display results from the three different perspectives (left, center and right) in Fig. 5(c) (i)-(iii), the relative position between the two objects '3' and 'D' indicates that the original 3D directional information can be retained with the proposed method for head tracking integral imaging display.

Fig. 6 presents the one dimensional intensity profiles along the yellow lines in Fig. 5(b) and (c) for comparison between the display results of the conventional and head tracking integral imaging. The blue dashed lines represent the intensity of the conventional 3D display, corresponding to Fig. 5(b). The pink lines represent the intensity of the head tracking 3D display, corresponding to Fig. 5(c). The comparison also shows that the head tracking 3D display quality has been improved for the large viewing angle from left and right perspectives in Fig. 6(a) and (c). If the viewing angle is within the acceptable field of view of the 3D display, both the conventional and head tracking integral imaging are able to provide high quality display results, as shown in Fig. 6(b).

Integral imaging is able to display 3D images with full parallax, and observers can accurately see the 3D scene from different perspectives. There may be cases such as mobile device displays or augmented reality displays when providing a rotated reconstructed image may be beneficial for the viewer. Another group of experiments was conducted for the case of a viewer with rotated head. The camera and the LED track clip were rotated with multiple degrees. Three groups of synthetic elemental images and the corresponding display results are shown in Fig. 7(a) and (b) for the head tracking 3D display with head rotation of 0°, 30° and 90°, respectively. The enlarged elemental images in Fig. 7(a), shows that with the image transformation in the simulated display, new set of elemental images with virtually rotated 3D information can be obtained.

Note that the proposed method is performed using computational pixel mapping between the captured elemental images and the synthetic elemental images. The algorithm does not require heavy computational calculations. The latency of the display system depends on the resolution of the display screen. In our experiments, the latency for the process of simulated display and synthetic capture is 12.5 seconds using Matlab which is not intended to be computationally efficient software. We used an Inter(R) i7 (CPU, 3.30 GHz) processor for our experiment. The latency of the system can be substantially improved by optimizing our code for real time implementation and by using GPU [33] or parallel processing for real time head tracking 3D display.

## V. CONCLUSION

In conclusion, a head tracking 3D integral imaging display for an extended viewing angle and 3D scene rotation is presented by implementing the pseudoscopic-to-orthoscopic conversion. A new set of elemental images corresponding to a specific viewing position can be generated by applying pixel mapping in the simulated display and synthetic capture stages. The crosstalk can be eliminated for a large viewing angle with the proposed system. By performing the rotation transformation in the simulated display, 3D scene displays can be achieved for rotated viewer head. Experimental results verify the feasibility of the proposed system.

## ACKNOWLEDGMENT

The authors would like to thank D. Nam and J. Park of Samsung SAIT for encouraging to work on this subject.

## REFERENCES

[1] B. Javidi, F. Okano, and J. Y. Son, *Three Dimensional Imaging, Visualization, and Display*. Berlin, Germany: Springer, 2009.

[2] G. Lippmann, "Epreuves reversibles donnant la sensation du relief," *J. Phys. Theor. Appl.*, vol. 7, no. 1, pp. 821–825, Nov. 1908.
[3] H. E. Ives, "Optical properties of a Lippmann lenticulated sheet," *J. Opt. Soc. Amer.*, vol. 21, pp. 171–176, 1931.
[4] C. Burckhardt, "Optimum parameters and resolution limitation of integral photography," *J. Opt. Soc. Amer.*, vol. 58, no. 1, pp. 71–74, Jan. 1968.
[5] T. Okoshi, "Three-dimensional displays," *Proc. IEEE*, vol. 68, no. 5, pp. 548–564, May 1980.
[6] L. Yang, M. McCormick, and N. Davies, "Discussion of the optics of a new 3-D imaging system," *Appl. Opt.*, vol. 27, no. 21, pp. 4529–4534, Nov. 1988.
[7] T. Inoue and H. Ohzu, "Accommodative responses to stereoscopic three-dimensional display," *Appl. Opt.*, vol. 36, no. 19, pp. 4509–4515, Jul. 1997.
[8] H. Hoshino, F. Okano, H. Isono, and I. Yuyama, "Analysis of resolution limitation of integral photography," *J. Opt. Soc. Amer. A*, vol. 15, no. 8, pp. 2059–2065, Aug. 1998.
[9] F. Okano, J. Arai, and M. Kawakita, "Wave optical analysis of integral method for three-dimensional images," *Opt. Lett.*, vol. 32, no. 4, pp. 364–366, Feb. 2007.
[10] X. Wang and H. Hua, "Theoretical analysis for integral imaging performance based on microscanning of a microlens array," *Opt. Lett.*, vol. 33, no. 5, pp. 449–451, Mar. 2008.
[11] A. Stern and B. Javidi, "3-D image sensing, visualization, and processing using integral imaging," *Proc. IEEE*, vol. 94, no. 3, pp. 591–607, Mar. 2006.
[12] R. Martinez-Cuenca, G. Saavedra, M. Martinez-Corral, and B. Javidi, "Progress in 3-D multiperspective display by integral imaging," *Proc. IEEE*, vol. 97, no. 6, pp. 1067–1077, Jun. 2009.
[13] X. Xiao, B. Javidi, M. Martinez-Corral, and A. Stern, "Advances in three-dimensional integral imaging: sensing, display, and applications," *Appl. Opt.*, vol. 52, no. 4, pp. 546–560, Jan. 2013.
[14] B. Javidi, J. Sola-Pikabea, and M. Martinez-Corral, "Breakthroughs in Photonics 2014: Recent advances in 3-D integral imaging sensing and display," *IEEE Photon. J.*, vol. 7, no. 3, pp. 1–7, Jun. 2015.
[15] C. W. Chen, M. J. Cho, Y. P. Huang, and B. Javidi, "Improved viewing zones for projection type integral imaging 3D display using adaptive liquid crystal prism array," *J. Display Technol.*, vol. 10, no. 3, pp. 198–203, Mar. 2014.
[16] R. Martínez-Cuenca, H. Navarro, G. Saavedra, B. Javidi, and M. Martinez-Corral, "Enhanced viewing-angle integral imaging by multiple-axis telecentric relay system," *Opt. Exp.*, vol. 15, no. 24, pp. 16255–16260, Nov. 2007.
[17] G. Park, J. Hong, Y. Kim, and B. Lee, "Enhancement of viewing angle and viewing distance in integral imaging by head tracking," in *OSA Tech. Dig. Adv. in Imaging*, 2009, paper DWB27.
[18] M. J. Cho, M. Daneshpanah, I. Moon, and B. Javidi, "Three-dimensional optical sensing and visualization using integral imaging," *Proc. IEEE*, vol. 99, no. 4, pp. 556–575, Apr. 2011.
[19] F. Okano, H. Hoshino, J. Arai, and I. Yuyama, "Real time pickup method for a three-dimensional image based on integral photography," *Appl. Opt.*, vol. 36, no. 7, pp. 1598–1603, Mar. 1997.
[20] J. Arai, F. Okano, H. Hoshino, and I. Yuyama, "Gradient-index lens-array method based on real-time integral photography for three-dimensional images," *Appl. Opt.*, vol. 37, no. 11, pp. 2034–2045, Apr. 1998.
[21] H. Navarro, R. Martínez-Cuenca, G. Saavedra, M. Martínez-Corral, and B. Javidi, "3-D integral imaging display by smart pseudoscopic-to-orthoscopic conversion (SPOC)," *Opt. Exp.*, vol. 18, no. 25, pp. 25573–2558, 3-Dec. 2010.
[22] M. Martínez-Corral, A. Dorado, H. Navarro, G. Saavedra, and B. Javidi, "Three-dimensional display by smart pseudoscopic-to-orthoscopic conversion with tunable focus,," *Appl. Opt.*, vol. 53, no. 22, pp. E19–E25, May 2014.
[23] X. Xiao, X. Shen, M. Martinez-Corral, and B. Javidi, "Multiple-planes pseudoscopic-to-orthoscopic conversion for 3d integral imaging display," *J. Display Technol.*, vol. 11, no. 11, pp. 921–926, Nov. 2015.
[24] H. Liao, M. Iwahara, N. Hata, and T. Dohi, "High-quality integral videography using multiprojector," *Opt. Exp.*, vol. 12, no. 6, pp. 1067–1076, Mar. 2004.
[25] F. Okano, J. Arai, K. Mitani, and M. Okui, "Real-time integral imaging based on extremely high resolution video system," *Proc. IEEE*, vol. 94, no. 3, pp. 490–501, Mar. 2006.
[26] J. Arai *et al.*, "Integral three-dimensional television using a 33-megapixel imaging system," *J. Display Technol.*, vol. 6, no. 10, pp. 422–430, Oct. 2010.
[27] J. H. Park, M. Y. Shin, and N. Kim, "Viewing direction controllable three-dimensional display based on integral imaging," in *SID Symp. Dig. Tech. Papers*, 2009, vol. 40, no. 1, pp. 607–610.
[28] H. Hua and B. Javidi, "A 3-D integral imaging optical see-through head-mounted display," *Opt. Exp.*, vol. 22, no. 11, pp. 13484–13491, June 2014.
[29] A. Schwartz, "Head tracking stereoscopic display," *IEEE Trans. Electron Devices*, vol. 33, no. 8, pp. 1123–1127, Aug. 1986.
[30] A. Stern, Y. Yitzhaky, and B. Javidi, "Perceivable light fields: Matching the requirements between the human visual system and autostereoscopic 3-D displays," *Proc. IEEE*, vol. 102, no. 10, pp. 1571–1587, Oct. 2014.
[31] X. Shen, X. Xiao, M. Martinez-Corral, and B. Javidi, "Format matching using multiple-planes pseudoscopic-to-orthoscopic conversion for 3-D integral imaging display," in *Proc. SPIE*, May 2015, vol. 9495, Three-Dimensional Imaging, Visualization, and Display 2015, 94950W.
[32] J. Jang and B. Javidi, "Three-dimensional synthetic aperture integral imaging," *Opt. Lett.*, vol. 27, no. 13, pp. 1144–1146, July 2002.
[33] F. Yi, I. Moon, J. A. Lee, and B. Javidi, "Fast 3-D computational integral imaging using graphics processing unit," *J. Display Technol.*, vol. 8, pp. 714–722, Dec. 2012.

**Xin Shen** received the B.S. degree in optical information science and technology from Xidian University, Xian, China, in 2010, and dual M.S. degrees, one M.S. degree in electronics and communication engineering from Xidian University in 2013, and one M.S. degree of Science in engineering from Doshisha University, Kyoto, Japan, in 2013. He is currently working toward the Ph.D. degree in electrical and computer engineering at the University of Connecticut, Storrs, CT, USA. His research interests include image processing, three-dimensional image reconstruction, 3D imaging, 3D display.

Mr. Shen is the event manager of the student chapter of the Optical Society of America (OSA) at the University of Connecticut.

**Manuel Martinez-Corral** received the Ph.D. degree in physics (Best Thesis Award) from the University of Valencia in 1993.

He is currently a Full Professor of optics at the University of Valencia, where he co-leads the "3D Imaging and Display Laboratory". His research interest includes resolution procedures in 3D scanning microscopy, and 3D imaging and display technologies. He has supervised on these topics 12 Ph.D. theses (three honored with the Best Thesis Award), published over eighty technical articles in major journals (which received approximately 1600 citations), and pronounced a number of invited and keynote presentations in international meetings.

Prof. Martinez-Corral is a Fellow of SPIE. He is co-chair of the Three-Dimensional Imaging, Visualization, and Display Conference within the SPIE meeting in Defense, Security, and Sensing, and Topical Editor of the IEEE/OSA JOURNAL OF DISPLAY TECHNOLOGY.

**Bahram Javidi** (S'82–M'83–SM'96–F'98) received the B.S. degree from George Washington University, and the M.S. and Ph.D. degrees from the Pennsylvania State University, all in electrical engineering.

He is the Board of Trustees Distinguished Professor with the University of Connecticut. He has over 900 publications, including nearly 400 peer reviewed journal article, over 400 conference proceedings, including over 110 plenary addresses, keynote addresses, and invited conference papers. His papers have been cited 29000 times according to the Google Scholar Citations $(\mathrm{h-index}=79)$. He is a coauthor on nine Best Paper Awards.

Dr. Javidi is a Fellow of the OSA and SPIE. In 2010, he was the recipient of The George Washington University's Distinguished Alumni Scholar Award, University's highest honor for its alumni in all disciplines. In 2008, he received a Fellow award by John Simon Guggenheim Foundation. He received the 2008 IEEE Donald G. Fink prized paper award among all (over 130) IEEE Transactions, Journals, and Magazines. In 2007, The Alexander von Humboldt Foundation awarded Dr. Javidi with Humboldt Prize for outstanding US scientists. He received the Technology Achievement Award from the SPIE in 2008. In 2005, he received the Dennis Gabor Award in Diffractive Wave Technologies from SPIE. He was the recipient of the IEEE Photonics Distinguished Lecturer Award twice in 2003–2004 and 2004–2005. He was awarded the IEEE Best Journal Paper Award from the IEEE TRANSACTIONS ON VEHICULAR TECHNOLOGY twice in 2002 and 2005. Early in his career, the National Science Foundation named him a Presidential Young Investigator and he received The Engineering Foundation and the IEEE Faculty Initiation Award. He was selected in 2003 as one of the nation's top 160 engineers between the ages of 30–45 by the National Academy of Engineering (NAE) to be an invited speaker at The Frontiers of Engineering Conference which was co-sponsored by The Alexander von Humboldt Foundation. He is an alumnus of the Frontiers of Engineering of The National Academy of Engineering since 2003. He serves on the Editorial Board of the Proceedings of the IEEE Journal [ranked #1 among all electrical engineering journals], the advisory board of the IEEE PHOTONICS JOURNAL, and he was on the founding board of editors of IEEE/OSA JOURNAL OF DISPLAY TECHNOLOGY.